Conductor Specification and Validation for High-Luminosity LHC Quadrupole Magnets

L. D. Cooley, *Senior Member, IEEE,* A. K Ghosh, D. R. Dietderich, and I. Pong

***Abstract*—The High Luminosity Upgrade of the Large Hadron Collider (HL-LHC) at CERN will replace the main ring inner triplet quadrupoles, identified by the acronym MQXF, adjacent to the main ring intersection regions. For the past decade, the U.S. LHC Accelerator R&D Program, LARP, has been evaluating conductors for the MQXFA prototypes, which are the outer magnets of the triplet. Recently, the requirements for MQXF magnets and cables have been published in P. Ferracin *et al., IEEE Trans. Appl. Supercond.*, vol. 26, no. 4, 2016, Art. no.4000207, along with the final specification for Ti-alloyed Nb_3Sn conductor determined jointly by CERN and LARP. This paper describes the rationale beneath the 0.85 mm diameter strand's chief parameters, which are 108 or more sub-elements, a copper fraction not less than 52.4%, strand critical current at 4.22 K not less than 631 A at 12 T and 331 A at 15 T, and residual resistance ratio of not less than 150. This paper also compares the performance for ~100 km production lots of the five most recent LARP conductors to the first 163 km of strand made according to the HL-LHC specification. Two factors emerge as significant for optimizing performance and minimizing risk: a modest increase of the sub-element diameter from 50 to 55 µm, and a Nb:Sn molar ratio of 3.6 instead of 3.4. The statistics acquired so far give confidence that the present conductor can balance competing demands in production for the HL-LHC project.**

***Index Terms*—Critical current, magnet conductors, Nb_3Sn, niobium tin superconductors, quadrupole magnets, residual resistance ratio, RRR.**

I. Introduction

THE QUADRUPOLE magnet triplets next to the main ring intersection regions of the Large Hadron Collider (LHC) will be upgraded during the High-Luminosity LHC (HL-LHC) upgrade, with installation scheduled to occur during the 2024–2026 shutdown [1]. Among the contributions by the United States, under the HL-LHC Accelerator Upgrade Project, will be 80 coils in 20 magnets, including spares, for the first and third magnets in the triplets, which are identical and are denoted as MQXFA. CERN will construct the inner, second magnets designated as MQXFB. Conductor production for these magnets should begin in 2017.

LARP is supported by the Office of High Energy and Nuclear Physics, U. S. Department of Energy, under contract No. DE-AC02-05CH11231 at Lawrence Berkeley National Laboratory; No. DE-AC02-07CH11359 at Fermi National Laboratory; and No. DE-AC02-98CH10886 at Brookhaven National Laboratory. Support by the High Luminosity LHC Project at CERN is also acknowledged.

L. D. Cooley is with Fermi National Accelerator Laboratory, Batavia, IL 80510 USA (e-mail: ldcooley@fnal.gov).

A. K. Ghosh, retired, was with Brookhaven National Laboratory.

I. Pong (e-mail: ipong@lbl.gov) and D. R. Dietderich, retired, (e-mail: drdietderich@lbl.gov) are with Lawrence Berkeley National Laboratory.

The U.S. LHC Accelerator R&D Program (LARP) has been developing prototype MQXFA magnets [2] leading up to the short model described in [3]. The magnets require 40-strand Rutherford cables manufactured from 0.85 mm diameter Nb_3Sn superconducting wire. The 4.2 m magnetic field length requires 455 m of cable, so 500 m of strand is re-spooled to accommodate cabling start-up, cabling parameters, samples and archive lengths. A single MQXFA cable thus requires 20 km of wire. Since a typical billet mass is about 45 kg, and the typical wire mass per unit length is about 5.0 kg•km^{-1}, a single piece of 0.85 mm wire can exceed 9 km in length. Cable fabrication will therefore require spools from 3 or more billets, which makes production uniformity important. Mitigation of risk for cable or coil failure requires the fabrication of extra cables to be included in the baseline plan. Production of 100 total cables is anticipated, which requires 2,000 km of wire and ~250 billets when manufacturing yield is taken into account, with total mass ~10 tons.

Specifications for magnets, cables, and conductor have been comprehensively reported in [3]. In this paper, we add detail to the discussion in [3] that describes the MQXF conductor specification, which applies to magnet conductor for both the U.S. and CERN. LARP developed several prior specifications as magnet needs evolved and as conductor manufacturing responded to those needs. These requirements were modified in early 2015 to increase margins for conductor manufacturing. We compare the initial data for MQXF strand to previous generations of LARP strand to evaluate whether in fact increased margins have been achieved. Included in the data are the initial 163 km of strand delivered to LARP under its final procurement leading up to the HL-LHC project, which was procured according to the HL-LHC strand specification summarized in [3]. These statistics suggest that the upcoming procurement for HL-LHC can be carried out with confidence.

II. Development of the Specification

A. Consideration of Trade-Offs

To date, LARP specifications have been met by Rod Restack Process (RRP) conductors manufactured by Oxford Instruments–Superconducting Technology (OST) [4]. The strand specifications have emphasized the following aspects:

- Strand critical current I_c measured at 12 T and 15 T field and 4.22 K temperature;
- Residual resistance ratio, RRR, evaluated as the ratio of resistance measured at 293 K to that measured just above the superconducting transition;
- Copper to non-copper ratio R or, equivalently, the

fraction of strand cross-section made up of copper;

- Sub-element diameter $d_s = 850\ [N\ (1 + R)]^{-0.5}$ in micrometers, where N is the number of sub-elements.

These aspects are inter-connected via the strand design and heat treatment schedule, such that simultaneous optimization of all properties has been difficult to achieve [4],[5].

Generally speaking, higher temperature and longer time of the final heat treatment stage tends to react more of the Nb and increase I_c, but also risks reduction of RRR [5],[6]. Reducing R allows more sub-elements to be included for higher I_c, but reduces magnet protection and stability. Reducing d_s reduces the threat of flux-jump instabilities and provides better field quality [7],[8], but high I_c has proven to be difficult to obtain reliably for $d_s < 50$ µm [4],[9],[10]. Recent 1.9 K magnet tests, [11] and strand magnetization measurements [12] gave confidence that d_s could be allowed to increase to 55 µm because magnetization flux-jump instabilities have small magnitude at 1.9 K. Alloying with Ti provides faster development of the Nb_3Sn layer at reaction temperatures of 635–665 °C than alloying with Ta [13],[14], making it possible to further restrict the reaction temperature to preserve high RRR. However, restricting the reaction temperature also yields values of the 4.2 K extrapolated upper critical field B_{c2}* of 25–26 T, somewhat below the highest values that can be obtained [14],[15]. This makes it more challenging to achieve high I_c at 15 T [6]. Reducing the ratio of tin to niobium has provided better control over RRR and flexibility for heat treatment schedule [4], but I_c can fall below the specified requirement if the reaction is too conservative.

B. Magnet Requirements

In late 2014, and carrying on during early 2015, the design of the MQXF triplet was modified slightly [2]. MQXFA magnets were lengthened from 4.0 m to 4.2 m, which reduced the requirement for transport current in the cable by about 5% to 16.5 kA at the 1.9 K operating point, equivalent to 413 A per strand. The peak field generated at this point is approximately 11.4 T. A requirement that magnets should be trained up to 108% of the operating current established the maximum value for current, 17.8 kA in the cable, equivalent to 445 A per strand. This complies with the 18 kA limit of power supplies.

Other changes allowed the degradation after cabling to increase from 3% to 5%. A temperature margin of more than 4.2 K was also required, which is equivalent to a current sharing temperature of not less than 6.1 K. These parameters map the magnet requirements onto a current-field plot, such as Fig. 4 of [3]. The MQXFA load curve can be parameterized as $B_{pk} = a\ I^{\,b}$ with $a = 0.00129$ T A^{-1} and $b = 0.936$, with I being the cable current. This intersects the operating point above.

C. Critical Current Specification

Several LARP conductors have been extensively analyzed according to strain scaling models [15]–[17]. This allows critical current measurements at 4.22 K and different magnetic fields to be extended to 1.9 K as well as up to the thermal margin. An important decision by the HL-LHC Accelerator Upgrade Project is to hold down testing costs by taking primary data at 4.22 K and using these scaling relationships to predict short-sample limits, with only spot testing at 1.9 K being planned. Good scaling fits were obtained with parameters identified in [15] and [16] for RRP strands, which require the following fitting parameters:

- Effective upper critical field B_{c2}*(0,0) = 27.8 T
- Effective critical temperature T_c* = 16.7 K
- Critical current pre-factor C* = 2033 A.

With these parameters, a critical surface at 4.22 K is defined by critical current values of 632 A at 12 T and 331 A at 15 T. These are reflected in Table I, as well as in [3]. The equivalent non-copper critical current density J_c values are 2450 and 1285 A•mm^{-2}, respectively. For a cable made from conductor at this minimum specification, the magnet load line at 1.9 K meets the ultimate limit at 21.5 kA. Allowing for 5% cable degradation determines a short-sample limit (SSL) of 21.2 kA at a field of 14.5 T. The operating point is then 78% of the SSL. At 11.4 T, the cable critical current is 34.7 kA, so the operating point is at 44% of this value. The current-sharing condition is reached at 6.7 K, indicating a temperature margin of 4.8 K and well above the requirement of 4.2 K.

Earlier LARP specifications used a 4.22 K critical state described by 684 A at 12 T and 362 A at 15 T, also shown in Table I. The equivalent J_c values are 2650 and 1400 A•mm^{-2}, respectively. For these parameters, the SSL is reached at

TABLE I
COMPARISON OF LARP SPECIFICATIONS AND CONDUCTORS

Quantity	MQXF Spec.	Previous LARP Specs.
	Round wires	
I_c (4.22 K, 12 T), A	≥ 632	684 info.
Equivalent J_c, A•mm^{-2}	2450 info.	2650 info.
I_c (4.22 K, 15 T), A	≥ 331	≥ 362
Equivalent J_c, A•mm^{-2}	1285 info.	1400 info.
R	1.2 ± 0.1	1.2 ± 0.1 [a]
d_s, µm	55 info.	≤ 50
N	≥ 108	
RRR	≥ 150	≥ 150
	Wires rolled to 0.72 mm flat-to-flat dimension [b]	
I_c (4.22 K, 12 T), A	≥ 600	663 (info.)
I_c (4.22 K, 15 T), A	≥ 314	≥ 350
RRR	≥ 100	≥ 100
	Conductor information	
Conductor type	Ti-alloyed Nb_3Sn	Ti-alloyed Nb_3Sn
Diameter and re-stack	0.85 mm 108/127	0.85 mm 132/169
		0.85 mm 144/169 [a]
		0.78 mm 108/127
Nb:Sn mol ratio	3.6:1	3.6:1 "5% reduced"
		3.5:1 "2.5% reduced" [a]
		3.4:1 "standard"
Reaction heat treatment	210 °C 48 h +	210 °C 48 h +
	400 °C 48 h +	400 °C 48 h +
	665 °C 75 h	650 or 665 °C, 48–50 h

Items labeled "info." are for information only, and are not requirements. The critical current density J_c is evaluated for the non-copper wire area. For MQXF strand, the sub-element diameter is *not* a requirement. Instead, the combination of strand diameter, N, and R define an average of 55 µm and facilitate quality control.

[a]The 144/169 conductor was manufactured with $R = 1.1 \pm 0.1$ and a 3.5:1 mol ratio of niobium to tin.

[b]The cable narrow edge dimension is 1.462 mm before reaction [3], which is approximated by 2 layers of the rolled strand thickness.

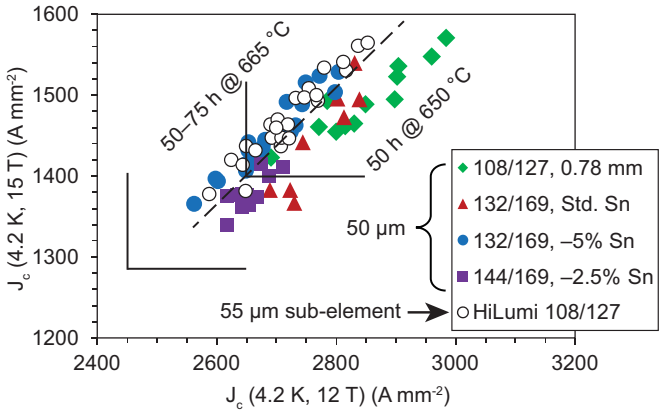

Fig. 1. Critical current density at 15 T is plotted vs. critical current density at 12 T, both at 4.2 K temperature. The vertical and horizontal lines represent the specifications listed in Table I. The diagonal dashed line separates data for conductors with a manufacturer's recommended heat treatment temperature of 665 °C from those with 650 °C.

21.8 kA and 14.6 T; slightly higher B_{c2}*(0,0) of 28.1 T and C* of 2143 A were used. The operating point prior to the MQXF review of 17.3 kA reaches 80% of the SSL, and has a current sharing temperature of 6.4 K.

III. Conductor Data

Critical current measurements from conductor quality control data are compared in Fig. 1 for the different conductors, with I_c(4.2 K,15 T) plotted against I_c(4.2 K,12 T). The data have not been corrected for bath temperature or self-field. Benchmarking efforts at different times revealed differences from 1.5% to 5.0% between measurements conducted at OST and LARP, with the lower results obtained by OST shown in the figure. The lines represent the critical current specifications. The dashed line divides the data points for reactions conducted at 650 °C from those at 665 °C.

In Fig. 2, the RRR is plotted against the I_c(4.2 K,15 T) data. The I_c data for the 0.78 mm strand have been scaled by 1.188 to adjust for the diameter difference compared to the other strands. These high-field data are most sensitive to the balance of heat treatment time and temperature with the configuration of the conductor and the molar ratio of niobium to tin. The lines represent the specifications in Table I.

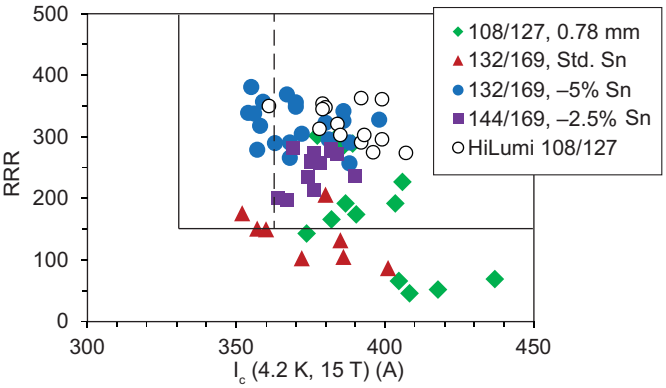

Fig. 2. RRR plotted vs. critical current at 15 T, 4.2 K. The vertical and horizontal lines denote the specifications listed in Table I. The critical current data for the 0.78 mm diameter 108/127 strand have been multiplied by $(0.85/0.78)^2 = 1.188$.

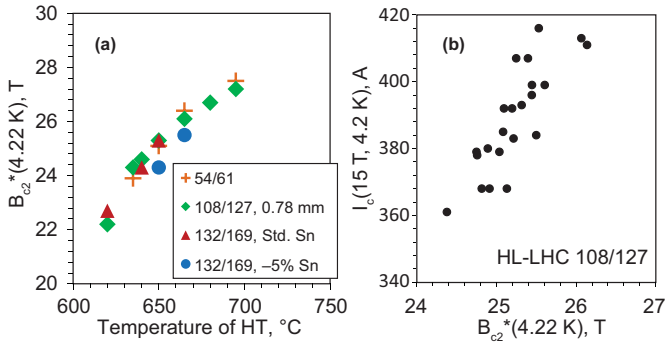

Fig. 3. Plot (a) shows the extrapolated scaling field for different LARP conductors with Ti doping, as a function of the temperature of the last heat treatment reaction stage. The reactions were 48 or 50 hours. Plot (b) shows the critical current at 15 T, 4.2 K for the HL-LHC strand vs. the extrapolated scaling field at 4.2 K. The reaction for this strand is 665 °C for 75 h.

Sensitivity to heat treatment time and temperature is emphasized further in Fig. 3. The value of B_{c2}*(4.2 K) where the flux-pinning force extrapolates to zero is plotted in Fig. 3(a) for different LARP conductors alloyed with Ti. In Fig. 3(b), I_c(4.2 K, 15 T) is plotted against B_{c2}*(4.2 K) for the HL-LHC strand. While a comprehensive study of B_{c2}*(4.2 K) as a function of reaction temperature for the HL-LHC strand is not available, the reader should note that the data in Fig. 3(a) spans a range of sub-element diameter and Nb:Sn ratio that encompasses the HL-LHC strand. The same trend should hold for HL-LHC strands, where the B_{c2}* values of Fig. 3(b) indeed lie upon the data shown in Fig. 3(a) at 665 °C. Taken together, these trends show that obtaining higher critical current at high field is connected with the ability to sustain a high temperature of the final stage reaction.

Fig. 4 shows conductor delivery statistics for orders that were more than 50 km total length. The HL-LHC MQXF strand data includes spools shipped to CERN with longer than 500 m strand on the spool. There are 63 spools represented in the HL-LHC data, covering 20 billets and 163 km total length. This converts to about 3.6 spools per billet on average, at 2.6 km average length. Also, an average of 8.16 km has been manufactured per billet, for 88% yield compared to the maximum of 9.25 km. These data are significantly higher than the corresponding data for the 132/169 and 0.78 mm 108/127 billets, especially for the increased fraction of strand at 3 km to 6 km length.

IV. Discussion

All of the different conductor types shown in Fig. 2 have coefficients of variation of the critical current between 3% and 4%, indicating high quality and consistency of the manufacturing process. By contrast, the coefficient of variation of RRR decreases as conductor generations improve, from 29% for the 0.78 mm strand to 10% for HL-LHC strand. This reflects how more focus on the multi-parameter optimization was given by OST [4], LARP [6],[8], the U.S. Conductor Development Program [18], and conductor development efforts worldwide [19].

Since the MQXFA conductor requirement is equivalent to about 250 billets, manufacturers that can replicate the LARP

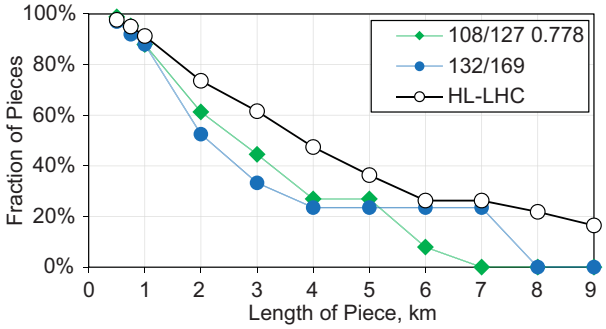

Fig. 4. Fraction of the total piece lengths for a particular conductor type plotted against length of conductor on the spool. A value of 50% at 2000 m means that half of the total conductor order was delivered with 2000 m or greater length on spools.

statistics could deliver the entire quantity comfortably above the specification. Based on the present data, the production run would be expected to lie between 342 and 429 A and RRR of 227 and 414, i.e. 3 standard deviations (99.7% coverage) above and below the average values of 386 A and 321 RRR.

The extra margin can be used for reduction of other risks associated with the cables and coils. For example, the present heat treatment recommendation for the cable and coil, 665 °C for 50 h, is somewhat more conservative than the manufacturer's recommendation for the strand, 665 °C for 75 h. Evaluation of strands extracted from the first cables manufactured using HL-LHC conductor showed that RRR can be kept above 200 at the locations corresponding to the cable edge using the 50 h heat treatment, with no apparent change in the critical current [20]. By contrast, using the manufacturer's recommended heat treatment results in some locations with RRR < 150. The specification for cables is RRR ≥ 100.

Two key factors in the conductor optimization appear to be reduction of the amount of tin relative to the amount of niobium, and improved sub-element uniformity. They allow longer reactions at 650 °C as well as reactions at 665 °C, thereby optimizing I_c with reduced risk for reduction of RRR. It is no coincidence that the HL-LHC conductor has the hottest and longest recommended reaction. Increasing the sub-element diameter from 50 µm, as for the 0.85 mm 132/169 design and the 0.778 mm 108/127 design, to 55 µm, as for the HL-LHC specification, may be an important decision in this regard. Fig. 4 shows that the conductors with 55 µm sub-elements have improved piece length, which may be an indicator of improved uniformity. The larger sub-element may also reduce losses associated with the formation of Cu-Nb-Sn inter-metallic phases during the heat treatment [9],[10],[14].

Fig. 1 shows the clear advantage for improving the critical current at 15 T relative to that at 12 T when the higher temperature is used for the final heat treatment. All of the data in Fig. 1 lie generally parallel to the dashed line, which reflects the scaling of flux-pinning behavior investigated by many researchers [15],[17],[21]. The data for 132/169 and HL-LHC conductors reflects an increase in B_{c2}* for these conductors. This point is made explicit in Fig. 3. Plot (a) shows how all of the RRP conductor types explored by LARP exhibit increase of B_{c2}*(4.2 K) with increasing reaction temperature. Included in this plot is data originally presented in [6]. Plot (b) shows that there is a direct dependence of I_c(15 T) on B_{c2}*(4.2 K).

Both the 132/169 and the HL-LHC conductor perform very well. However, their cost and manufacturing are different. Fig. 4 shows how the HL-LHC conductor can be delivered in longer lengths, on average, than the 132/169 conductor. Long pieces improve efficiency of use for cabling, called "mapping yield", because the remnant, after dividing the piece into many equal units for re-spooling on the cabling machine, is a smaller fraction of the initial piece. If the manufacturer is required to deliver whole units, as is the case for the HL-LHC project, then these remnants are material losses that would be covered by an increased price. At the present 3.6 pieces per billet average, and with a 0.25 km remnant per piece, the mapping yield is about 91%. Thus, a manufacturer could be expected to propose a price inflated by 9% to cover this waste. This would be in addition to any inflation that covers the manufacturing yield, presently about 88% for LARP and HL-LHC strands.

V. Conclusions

The recommendations extending from the MQXF review in late 2014 sought to increase margin for the HL-LHC conductor. This resulted in a change in the HL-LHC conductor specification, which was enacted in May 2015, as summarized in [3]. Between 2015 and the present, conductor has been delivered according to the HL-LHC specification in a quantity approximately one-tenth of the scale of the full procurement for the HL-LHC Accelerator Upgrade Project. This has provided adequate statistics to evaluate whether the new specification has produced the changes recommended.

The conductor data analyzed so far indicates improvement relative to the performance of past LARP conductors. High critical current and high RRR can be simultaneously obtained, in part due to benefits of the 5% reduced tin conductor design, because reaction temperatures at 665 °C can be used without significantly jeopardizing the simultaneous optimization of critical current and RRR. The higher reaction temperature, compared to 650 °C used in past LARP conductors, results in higher values of the effective upper critical field B_{c2}*, which directly translates to a higher critical current at the 15 T specification point. Allowing the sub-element diameter to increase slightly, from 50 to 55 µm, may also contribute to longer piece length and better control over the reaction.

The improved critical current and RRR for the HL-LHC conductor exhibits a statistical spread that has significant margin above the specification limits. Considering zones that are 3 standard deviations above and below the average values of I_c and RRR, which is a coverage of 99.7%, the LARP procurement still has a margin of about 3% over the critical current and 30% over RRR. If the ~250 billet HL-LHC manufacturing effort achieves the same statistics, then all delivered pieces would be expected to come in safely above the requirements.

Acknowledgment

We thank B. Bordini for providing piece length information

for HL-LHC strands received by CERN.

REFERENCES

[1] Giorgio Apollinari, Lucio Rossi, and Oliver Brüning, "High Luminosity LHC Project Description," CERN-ACC-2014-0321, May, 2014.

[2] S. Izquierdo Bermudez, G. Ambrosio, A. Ballarino, E. Cavanna, R. Bossert, D. Cheng, D. Dietderich *et al.* "Second-Generation Coil Design of the Nb_3Sn low-Quadrupole for the High Luminosity LHC," *IEEE Trans. Appl. Supercond.*, vol. 26, no. 4, 2016, Art. no. 4001105.

[3] P. Ferracin *et al.*, "Development of MQXF: The Nb_3Sn Low-β Quadrupole for the HiLumi LHC," *IEEE Trans. Appl. Supercond.*, vol. 26, no. 4, 2016, Art. no.4000207.

[4] M. B. Field, Y. Zhang, H. Miao, M. Gerace, and J. A. Parrell, "Optimizing conductors for high field applications," *IEEE Trans. Appl. Supercond.*, vol. 24, no. 3, 2014, Art. no. 6001105.

[5] C. Tarantini, P. J. Lee, N. Craig, A. Ghosh, and D. C. Larbalestier, "Examination of the trade-off between intrinsic and extrinsic properties in the optimization of a modern internal tin Nb_3Sn conductor," *Supercond. Sci. Technol.*, vol. 27, no. 6, 2014, Art. no.065013.

[6] A. K. Ghosh, E. A. Sperry, J. D'Ambra, and L. D. Cooley, "Systematic changes of the Nb-Sn reaction with time, temperature, and alloying in restacked-rod-process (RRP) strands," *IEEE Trans. Appl. Supercond.*, vol. 19, no. 3, pp. 2580–2583, 2009.

[7] L. D. Cooley, P. S. Chang, and A. K. Ghosh, "Magnetization, RRR and Stability of Nb_3Sn strands with high sub-element number," *IEEE Trans. Appl. Supercond.*, vol. 17, no. 2, pp. 2706–2709, 2007.

[8] A. K. Ghosh, E. A. Sperry, L. D. Cooley, A. M. Moodenbaugh, R. L. Sabatini, and J. L. Wright, "Dynamic stability threshold in high-performance internal-tin Nb_3Sn superconductors for high field magnets," *Supercond. Sci. Technol.*, vol. 18, no. 1, pp. L5–L8, 2004.

[9] Ian Pong, Luc-Rene Oberli, and Luca Bottura, "Cu diffusion in Nb_3Sn internal tin superconductors during heat treatment," *Supercond. Sci. Technol.* vol. 26, no. 10, 2013, Art. no. 105002.

[10] C. Sanabria, P. J. Lee, and D. C. Larbalestier, "The vital role of a well-developed Sn-Nb-Cu membrane for high J_c RRP Nb_3Sn wires," *IEEE Trans. Appl. Supercond.*, submitted for publication.

[11] H. Bajas *et al.,* "Cold Test Results of the LARP HQ Quadrupole Magnet at 1.9 K," *IEEE Trans. Appl. Supercond.*, vol. 23, no. 3, 2013, Art. no. 4002606.

[12] B. Bordini, D. Richter, P. Alknes, A. Ballarino, L. Bottura, and L. Oberli, "Magnetization Measurements of High-J_c Nb_3Sn Strands," *IEEE Trans. Appl. Supercond.*, vol. 23, no. 3, 2013, Art. no. 7100806.

[13] A. K. Ghosh, L. D. Cooley, J. A. Parrell, M. B. Field, Y. Zhang, and S. Hong, "Effects of Reaction Temperature and Alloying on Performance of Restack-Rod-Process Nb_3Sn," *IEEE Trans. Appl. Supercond.*, vol. 17, no. 2, pp. 2623-2626, 2007.

[14] C. Tarantini, Z. H. Sung, P. J. Lee, A. K. Ghosh, and D. C. Larbalestier, "Significant enhancement of compositional and superconducting homogeneity in Ti rather than Ta-doped Nb_3Sn," *Appl. Phys. Lett.*, vol 108, no. 4, 2016, Art. no. 042603.

[15] A. Godeke, "A review of the properties of Nb_3Sn and their variation with A15 composition, morphology and strain state," *Supercond. Sci. Technol.*, vol. 19, no. 8, pp. R68–R80, 2006.

[16] D. Arbelaez, A. Godeke, and S. O. Prestemon, "An improved model for the strain dependence of the superconducting properties of Nb_3Sn." *Supercond. Sci. Technol.*, vol. 22, no. 2, 2008, Art. no. 025005.

[17] Jack W. Ekin, Najib Cheggour, Loren Goodrich, Jolene Splett, Bernardo Bordini, and David Richter, "Unified scaling law for flux pinning in practical superconductors: Part 2. Parameter testing, scaling constants, and the extrapolative scaling expression," *Supercond. Sci. Technol.* vol. 29, no.12, 2016, Art. no. 123002.

[18] D. R. Dietderich, and A. Godeke. "Nb_3Sn research and development in the USA–Wires and cables," *Cryogenics*, vol. 48, no. 7, pp. 331-340, 2008.

[19] Amalia Ballarino, and Luca Bottura. "Targets for R&D on Nb_3Sn Conductor for High Energy Physics," *IEEE Trans. Appl. Supercond.*, vol. 25, no. 3, 2015, Art. No. 6000906.

[20] A. K. Ghosh, Brookhaven National Laboratory (retired), unpublished result, presented at the 26th LARP Collaboration Meeting, SLAC National Accelerator Laboratory, Stanford, CA, USA, May 2016.

[21] J. W. Ekin, "Unified scaling law for flux pinning in practical superconductors: I. Separability postulate, raw scaling data and parameterization at moderate strains," *Supercond. Sci. Technol.* vol. 23, no. 8, 2010, Art. no. 083001.